3D ODZIV IZKOPA VAROVANEGA Z NAGNJENIMI OPORNIKI V BLIŽINI ZGRADB

Zahra Sabzi *(vodilni avtor)*
Karaj branch, Islamic Azad University,
Department of Engineering
Karaj, Iran
E-pošta: zahra.sabzi@kiau.ac.ir

Ali Fakher
University of Tehran,
Faculty of Engineering
Teheran, Iran
E-pošta: afakher@ut.ac.ir

Ključne besede

izkop, nagnjen opornik, sosednja zgradba, terenska meritev, 3D analiza s končnimi elementi, projektiranje na osnovi pomikov

Izvleček

Predstavljena študija se osredotoča na terenska opazovanja in 3D numerične analize izkopa, varovanega z nagnjenimi razporami v bližini zgradb. Raziskan je učinek opornikov na prenašanje obtežb in zmanjšanje upogibov. Oporniki zmanjšujejo vrednosti deformacij in ustvarijo tudi kotni učinek podoben kot v vogalu diafragm. Raziskovan je vpliv razdalje med oporniki in predlagan optimalni razmik med oporniki. Predlagana je najbolj učinkovita konfiguracija vgradnje opornikov za zmanjševanje deformacij in poškodb zgradbe. Na podlagi rezultatov numeričnih študij so predstavljene smernice za projektiranje na osnovi pomikov.

3D RESPONSE OF AN EXCAVATION ADJACENT TO BUILDINGS SUPPORTED BY INCLINED STRUTS

Zahra Sabzi *(corresponding author)*
Karaj branch, Islamic Azad University,
Department of Civil Engineering
Karaj, Iran
E-mail: zahra.sabzi@kiau.ac.ir

Ali Fakher
University of Tehran,
Faculty of Engineering
Teheran, Iran
E-mail: afakher@ut.ac.ir

Keywords

excavation, inclined strut, adjacent building, field measurement, 3D finite-element analysis, displacement-based design

Abstract

The presented study focuses on field observations and a 3D numerical analysis of open-cut excavations adjacent to a building supported by inclined struts. The performance of the struts in carrying the building loads and decreasing the deflections is investigated. Struts reduce the amount of deformations and also create a corner effect similar to the diaphragm walls corner. The influence of the distance between the struts is studied and the optimum struts interval is proposed. The most effective configuration of struts installation in reducing the deflections and building damage is proposed. A displacement-based design guideline is also presented based on the results of numerical studies.

1 INTRODUCTION

A simple method for protecting the buildings adjacent to open-cut excavations is the use of inclined struts connected to the buildings. This method is considered as a traditional support method in Iran and is the most common method in small-sized excavations [1]. Fig.1 schematically illustrates the use of struts and the current state-of-the-practice for this method. In the presented method, which is appropriate for a small to medium depth of excavations, the struts are directly connected to the buildings and control the movements of the buildings and consequently reduce the soil movements. The method is the subject of this paper and should not be mistaken for the use of struts that are connected to the retaining walls. Some studies were conducted and the primary understanding of the performance of inclined struts was presented [2], [3]. The performance mechanisms of such a strut were proposed as follows: (i) the load of the adjacent building is partially passed to the bottom of the excavation through the strut and consequently less pressure is exerted on the soil beneath the foundation; therefore, the settlement of the foundation decreases. (ii) The strut reduces the horizontal displacements of the buildings due to the lateral constraints it creates. Consequently, it can reduce the horizontal deflections of the excavation unsupported face. The deformation pattern of the excavation face and the ground surface settlement were strongly affected by the use of inclined struts that are connected to the building. Previous studies on this method showed that the use of inclined struts that are connected to the adjacent buildings influences the deformation patterns; the shape of the horizontal deflection at the excavation face is changed from cantilever type to lateral-bulging type; the ground surface settlement profile is changed from spandrel-type to concave-type [3].

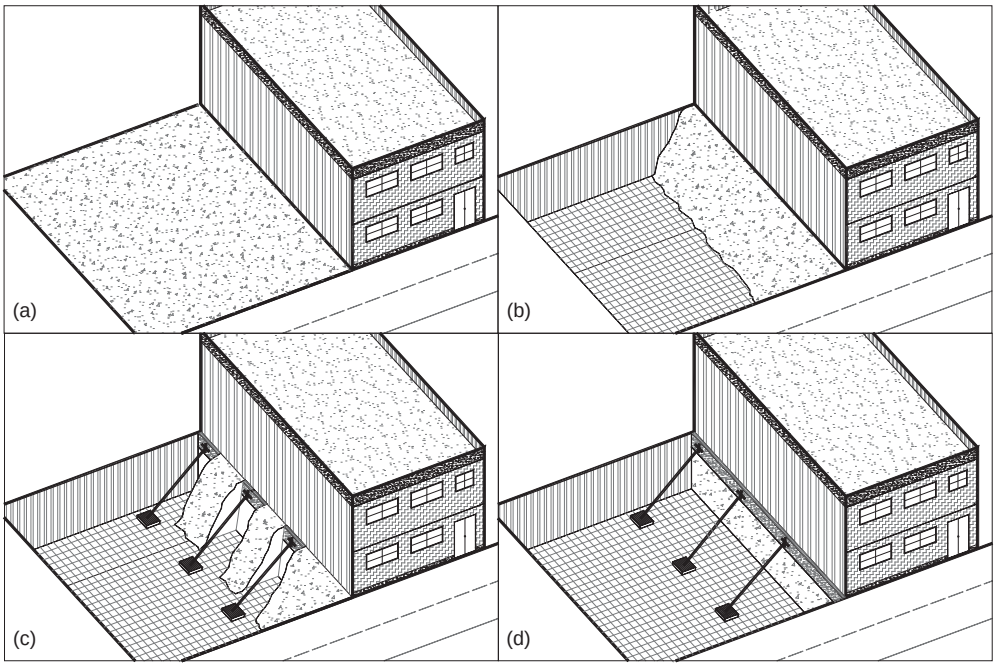

Figure 1. Schematic of the current state-of-the-practice of excavation using inclined struts connected to an adjacent building (a) before excavation; (b) excavation stage 1; (c) installation of struts, stage 2; (d) excavation stage 3.

One of the objectives of this paper is to verify the proposed mechanisms of struts through 3D numerical analyses and a comparison of field measurements and numerical studies.

Fig. 2 shows the most conventional configurations for excavation. Sadeghian and Fakher presented the most effective configuration for strut installation that produces the least ground surface settlement and horizontal deflection [2].

In this pattern the struts install after the first stage of excavation by sloping the sides of the excavation and then excavating the marginal soil behind the struts (Fig.2 (e)). This configuration minimizes the damage to the buildings, according to the criteria proposed by [4].

Sadeghian and Fakher obtained optimum results for inclined strut installation by connecting the struts to the

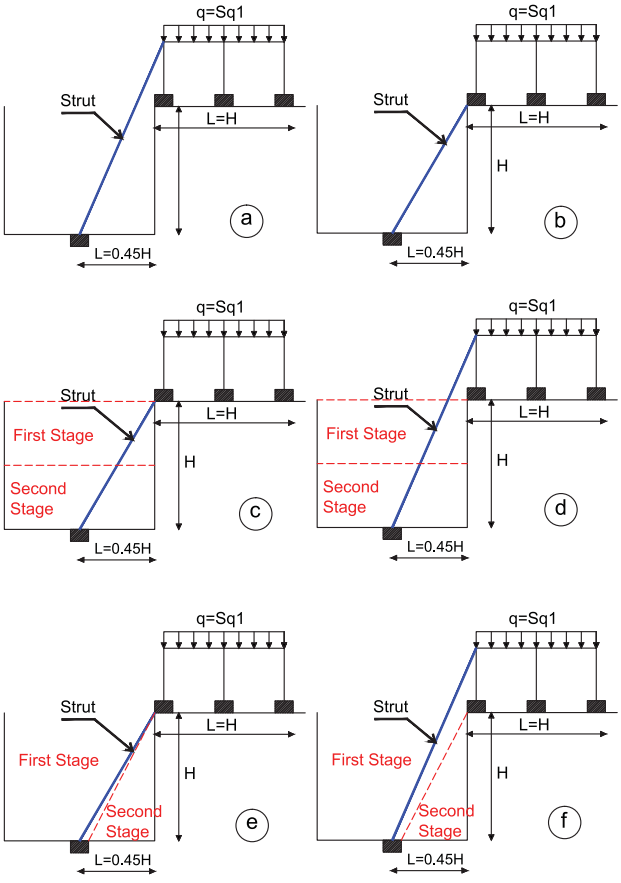

Figure 2. Most common configurations of the excavation procedure using inclined struts. (a) Struts connected to the first floor after full excavation. (b) Struts connected to the foundation after full excavation. (c) Struts connected to the foundation after full excavation made in two stages. (d) Struts connected to the first floor after full excavation, made in two stages. (e) Struts connected to the foundation after the first stage of excavation. (f) Struts connected to the first floor after the first stage of excavation [2].

foundation of the adjacent building [2]. Fig. 2 illustrates the most effective inclination angle for the struts at L/H = 0.45, where L is the distance of the struts from the excavation face at the bottom and H is the excavation depth. This value corresponds to an inclination angle of 65° above the horizontal.

Failure to control the deformations can cause significant damage to adjacent structures. Consequences such as the loss of bearing capacity of the foundations of adjacent building and the loss of a factor of safety for basal heave, global instability or bearing capacity can become very hazardous. In the presented paper, it is assumed that the safety factor of excavation is in an acceptable range that is derived from an appropriate limit equilibrium analyses or design codes (e.g., The National Building Regulations of Iran suggest safety factors for basal heave, global instability or bearing capacity for different conditions and depths of excavations). Thus, the presented analyses are focused on the displacements induced by the excavation and on the assessment of the admissibility of these displacements with respect to the maximum acceptable values.

Although the mentioned method has many practical applications, the inclined struts' behavior is not fully understood and determinations of the design parameters like loads and the distance between the struts are uncertain. Most designs are based on past experiences and no definitive conclusions exist regarding the effect of the struts on the deformations.

Two-dimensional plane-strain finite-element analyses of the strutted excavation have been performed by many researchers [5], [6], [7], [8],[9], [10]. But excavations behave as a three- dimensional problem [11]. Many studies have been performed to investigate the three-dimensional performance of excavations [12], [13], [14], [11], [15], [16], [17]. The mentioned method of excavation using inclined struts has been previously analyzed using 2D finite-element modeling [1], [2], [3], [18], but some important aspects can be simulated only when a 3D model is employed. Among them: (i) the behavior of the excavation corners, (ii) the sequence of struts installation and (iii) the struts interval can be mentioned. In this study, a series of parametric studies using a 3D numerical model were performed to examine the struts' performance.

2 NUMERICAL ANALYSIS

In the presented research, three-dimensional analyses were performed to account for the complex 3D nature of the excavation and to examine the inclined struts in the excavation. Numerical simulations were carried out using the FEM program ABAQUS [19]. Fig. 3 shows the finite-element mesh. The soil was modeled using three-dimensional brick elements with eight nodes. A large zone was selected to avoid any measurable effects from the boundaries. It was assumed that the vertical boundary is free in the vertical direction and restricted in the horizontal direction; and the bottom horizontal boundary was restricted in both the horizontal and vertical directions. To minimize the boundary effects, the vertical boundary and the bottom horizontal boundary at the far ends were set to almost 5 times the excavation's width and depth, from the center of the excavation.

The element size is chosen based on the desire to increase the accuracy of the results and reducing the computational effort. A large number of iterations were carried out to achieve the convergence criteria and the accuracy of the deflections. In a finite-element simulation of excavations it has been demonstrated that the refinement of the mesh had no significant effect on the final displacements [20]

In this study the horizontal dimensions were set to be of the same order as the vertical dimension and to be compatible with the dimensions of the excavated area. In order to reduce the required computational effort, the element dimensions could increase as the distance from the excavated area increases.

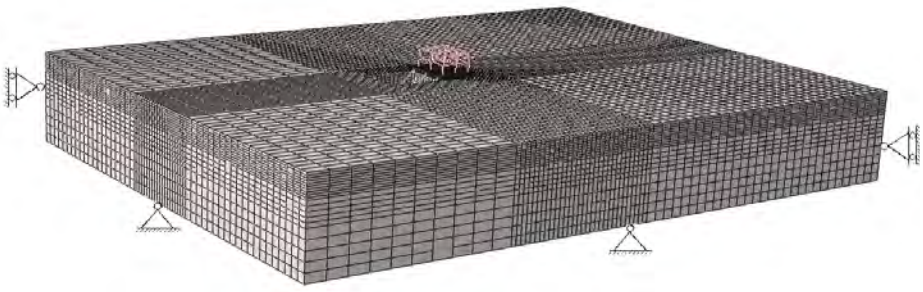

Figure 3. Finite-element mesh used in the analysis.

Many soil models in the literature can represent the excavation, but as the objective of the presented paper is to study the effect of struts, a simple model may be more illustrative than a complex one. In this study, the nonlinear elasto-plastic behavior of soils is simulated using the hyperbolic model [21]. The hyperbolic model is implemented with a user-defined model within the subroutine UMAT in the ABAQUS program and then used in the analyses. Although the hyperbolic model is not formulated based on the theory of plasticity, it considers the deformation characteristics of soils such as the nonlinear, inelastic, and strain-dependent ones. The hyperbolic model has been used in analyzing excavation problems [12], [14], [22], [23], [24], [25] possibly due to the fact that this type of soil model is relatively simple, conceptually understood, and easy for determining the soil parameters [12].

For the hyperbolic model, seven parameters are required to fully describe the stress–strain behavior of the soil. These are cohesion (c), friction angle (ϕ), stiffness modulus number for primary loading (E), stiffness modulus exponent (m), stiffness modulus number for unloading–reloading (E_{ur}), failure ratio (R_f), and Poisson's ratio (v).

3 VALIDATION OF THE NUMERICAL MODEL

The built numerical model in the current study was validated using data obtained from a field measurement undertaken by the authors. Then extensive parametric studies were performed to evaluate the trend of excavation behavior with respect to the variation of parameters.

3.1 Project description

Three boreholes were drilled in order to investigate the soil properties required for modeling the excavation. The soil at the excavation site typically consisted of marl that contains variable amounts of clays and silts and was plastic and sticky. Fig. 4 shows the stratigraphy of the site's soil. As shown in Fig.4 the subsurface conditions at the site consisted of two layers. The first layer was about 8m-thick stiff clayey silt; and this layer mainly affected the excavation behavior. The second layer was about 10m-thick stiff silty clay. No groundwater table was detected in the excavation zone; this means that pore water pressure had no effect on the behavior of the excavation. Fig.4 also shows variations of standard penetration test number (N_{SPT}) and the strength parameters of the soil. The shear-strength parameters were obtained from triaxial tests. The unit weight of the soil layers are also given in Fig.4.

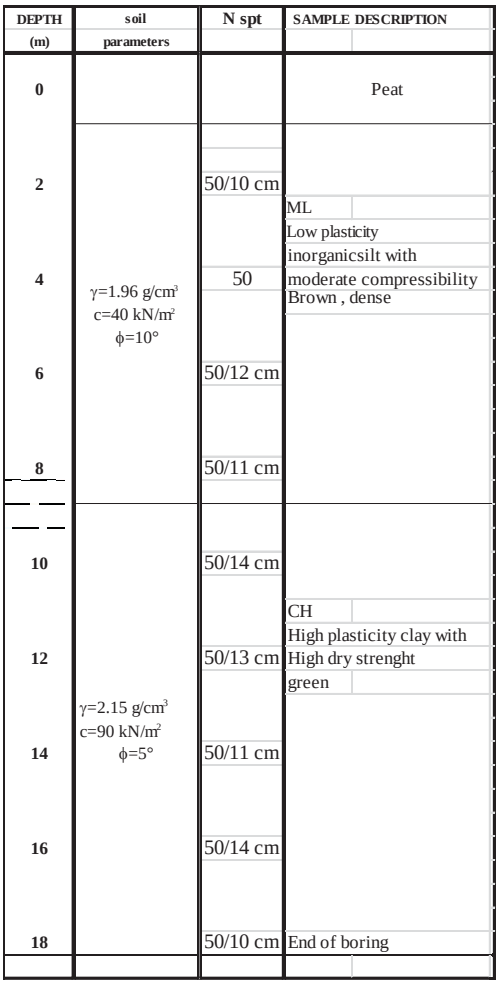

Figure 4. Stratigraphy of the excavation case.

A plan view of the dimensions of the excavation, support system geometry, neighboring structures and the instrumentations are shown in Fig. 5. As shown in this figure, the shape of the excavation site was 10×16 m^2. The final excavation depth was 4.5m, and this was completed using the described method, which is illustrated in Fig.1. The inclination of the struts was about 45° due to the site condition and the working space. The foundation of the neighboring building was mat footing. To monitor the displacements, optical survey points on the excavation face and buildings were used. Electrical strain gauges and a mechanical load cell, which was designed and fabricated by the authors, were used to measure the strut loads. The excavation procedure and strut-installation sequences are given in Table 1.

The dimensions of the structural elements in a building and the struts in numerical model were the same as for the excavation case. The neighboring building on the north side of the excavation was a three-story

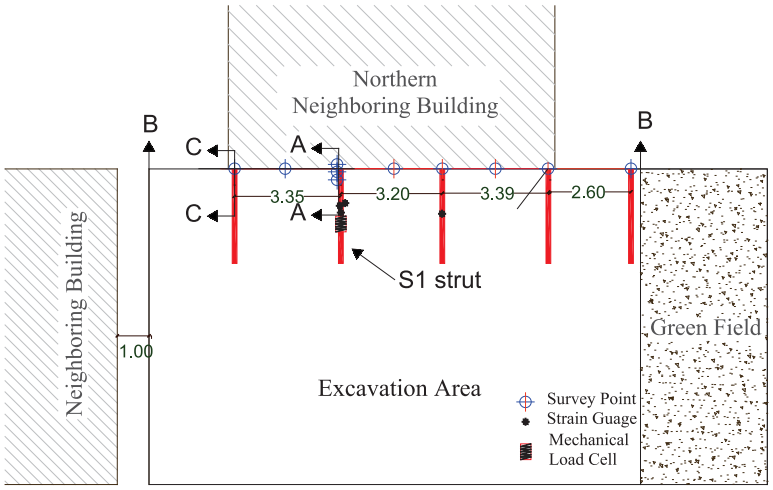

Figure 5. Plan view of excavation and instrumentation scheme.

Table 1. Excavation phases of the project.

Excavation stages	Description
1	Excavate down to 4.5 m below the ground surface by sloping the sides of excavation as shown in Fig.1 (b).
2	Construction of the foundation of the struts and installation of the struts, Fig.1 (c).
3	Excavation of marginal soil behind the struts, Fig.1 (d).

structure and was modeled as a steel frame by using beam elements as linear elastic materials with no failure criterion and the Young's modulus of steel was set $E_{steel} = 2.0\times10^5$ MPa. The inclined struts, that were connected to the adjacent building foundation, were steel box 140×140×7mm^3 and were modeled using three-dimensional beam elements and were simulated as linear elastic materials with no failure criterion and the Young's modulus is set to $E_{steel} = 2.0\times10^5$ MPa. The concrete foundations of the struts were 500 ×500 mm^2 bearing pads with a 400 mm thickness, which were placed below the ground level of excavation, but were modeled as a single mat foundation due to the negligible effect on results. The foundation of the building and the foundation of the struts were modeled as concrete foundations using solid elements as linear elastic material with no failure criterion and the Young's modulus of concrete was set $E_{concrete} = 2.0\times10^4$ MPa. The interface between the structure and the soil elements was modeled using contact elements.

The geotechnical characteristics of soil are presented in Table 2. The strength parameters c and ϕ were obtained directly from Drained and Consolidated (CD) triaxial laboratory tests. The value of the Young's modulus of first layer at a depth of 2 m of soil was directly obtained from the plate load-test results and provides a primary understanding of the soil stiffness. Table 3 lists the parameters of the geometry of the excavation used in the numerical analyses. The struts spacing are as shown in Fig.5.

In this study the soil stiffness modulus parameters (K, K_{ur}) are estimated from the plate load-test results and verified by the stiffness of soil of a nearby similar excavation project. The failure ratio, R_f, is normally in the range 0.5 and 1.0 [26]. In this study, R_f is assumed to be 0.9 for cohesive soil, accounting for the flexible behavior of clay [26]. The stiffness modulus exponent, m, can reasonably be assumed to be 0.5 for the cohesionless soil [27] and m should be equal to 0.0 for cohesive soil due to the concept of effective stress [27]. Poisson's ratio is assumed to be 0.3 at the pre-failure condition and 0.49 at or near the failure condition. The lateral earth pressure at rest, K_0, is obtained from Jaky's equation.

Table 2. Parameters of the soil used in numerical modeling.

Parameter	K	K_{ur}	m	c (kPa)	$\phi°$	γ(kN/m^3)	R_f	$v_{prefailure}$	$v_{failure}$	K_0
Layer 1	1900	4300	0.3	40	10	19.6	0.9	0.3	0.49	0.82
Layer 2	2550	5500	0.1	90	5	21.5	0.9	0.3	0.49	0.91

Note:K, K_{ur}, c, ϕ, m, R_f, v : the hyperbolic model parameters; K_0= "at-rest" coefficient of lateral earth pressure.

Table 3. Parameters of the excavation project used in the numerical modeling.

Parameter	H (m)	B (m)	L (m)
Amount	4.5	10	16

Note: H= excavation depth, B= excavation width and L= excavation length.

3.2 Excavation-induced displacements and loads

Figs. 6, 7 and 8 show the observed deflections at excavation stages and show the comparison of the deflections between the field observations along the north side of the excavation and the FE model predictions.

By comparing the results for excavation with and without struts, the effectiveness of the struts can be evaluated. Fig.6 shows that the computed horizontal deflections of the excavation face at section A-A (Fig.5), for three stages are much smaller than those without struts. It can be seen that the maximum horizontal deflection at the analysis is reduced by 50%, by the installation of strut. Also, it can be seen from Fig.6 that the use of struts connected to the adjacent building

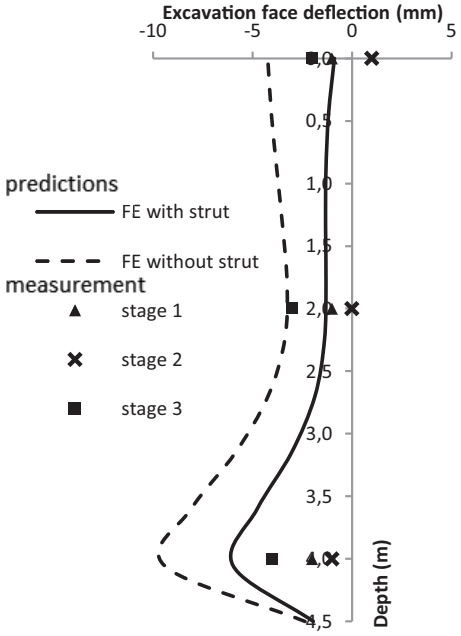

Figure 6. Comparison of the measured horizontal deflections and finite-element (FE) analyzed values for the excavation face at section A-A, shown in Fig.5.

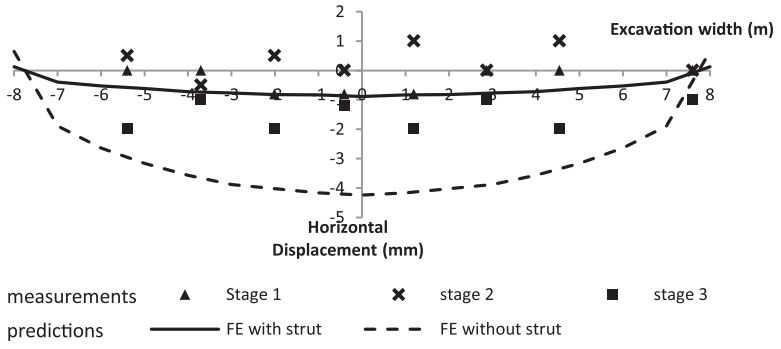

Figure 7. Comparison of the measured horizontal deflections and finite-element (FE) analyzed values along the north side of the excavation; section B-B shown in Fig.5.

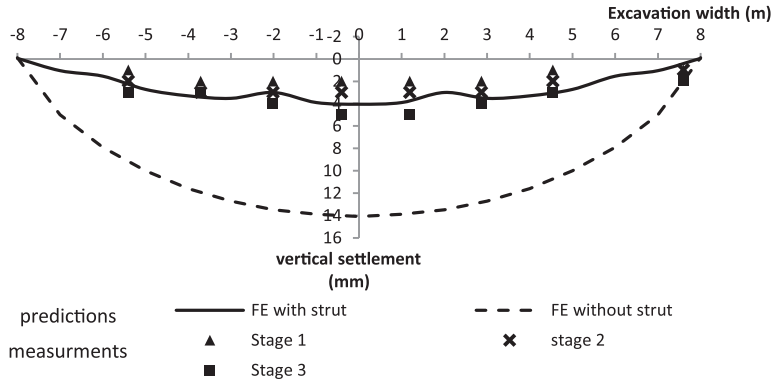

Figure 8. Comparison of the observed vertical settlements and finite-element (FE) analyzed values along the north side of the excavation; section B-B shown in Fig.5.

decreased the horizontal deformation to a slight value near the excavation surface around the contact point of the strut and lowered the location of the maximum horizontal deformation near the excavation bottom, whereas without using the struts, a large horizontal deformation will occur near the excavation surface.

Similarly, Figs.7 and 8 show that the computed horizontal deflections and surface settlements of the foundations along the north side (i.e., section B-B in Fig.5) for three stages are much smaller than those without struts. The maximum horizontal deflection and the vertical settlement beneath the foundation along the north side are reduced by about 80% and 70% respectively due to the installation of struts. Therefore, the installation of struts can substantially reduce the lateral deflections and vertical settlements.

Moreover in Figs.7 and 8, it is clear that there is a larger zone of relatively constant horizontal deflection and vertical settlements at the end of stage 1 than at the end of stage 3. This means that before the installation of strut, the plane strain condition exists over a larger portion of the excavation length than after the installation of a strut, where a shallower section has relatively constant values; and the 3D effects of the excavation become more apparent as the struts are installed.

Figures show that the computed deflections for the excavation with the strut are reasonably consistent with those observed in field measurements. Therefore, it is found that the above-mentioned numerical model is able to predict the deflections of the excavations.

As stated in the introduction of the presented paper, the performance mechanism of the struts derived from the field measurements and the 2D numerical analysis. It is needed to quantify in detail the 3D performance of the struts in excavations to provide a reasonable method to design the struts.

The ground surface settlement profile and the horizontal deflection of the excavation face illustrate the restraining effect of the struts on soil movement. The results of the numerical analysis make it clear that the struts decrease the horizontal displacements of the excavation face. The vertical settlement is also reduced by the installation of struts. These results confirm the mechanisms (i) and (ii). Moreover, it can be seen from Figs. 7, 8 that the maximum horizontal deflection and vertical settlement occur at the approximate middle position of the excavation length. Also, as shown from field observations in Figs.7 and 8, the horizontal deflection and vertical settlement are smaller at the section where struts are installed than those sections at a distance from the struts.

Fig. 9 illustrates the lateral deflection of the excavation face derived from numerical analyses at different positions of the excavation length (Fig.5.) The maximum horizontal movements occur near the bottom of the excavation at the center of the excavation length and much smaller lateral movements occur at the corners. It can be seen that the 3D effects become more apparent as the excavation depth increases, confirming that the effects of the corners of the excavation become more apparent as the horizontal deflection increases.

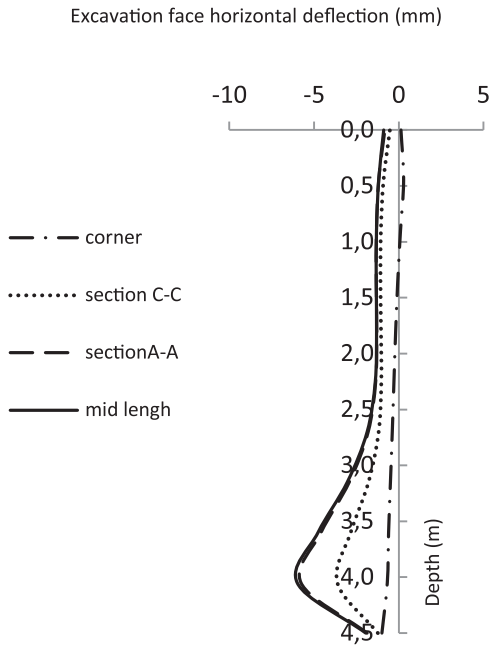

Figure 9. Comparison of the lateral movements of different positions of the excavation length (as shown in Fig.5).

4 INVESTIGATION OF THE 3D BEHAVIOR OF EXCAVATION

In this section the effects of important parameters are studied using the above-mentioned 3D finite-element model. A large number of finite-element analyses are made to evaluate the influence of the geometry of excavation and the parameters of the struts on the deformations. The results of the parametric studies are summarized herein.

4.1 3D effect of struts

In this section the values for H, B, L and the strut spacing were changed, as shown in Table 4, to investigate the effects of the various parameters in the parametric studies. Fig. 10 shows a cut of the 3D model in detail, to obtain a better understanding of the results.

Table 4. Parameters used in the parametric studies.

Parameter	H (m)	B (m)	L (m)	d (m)
Amount	4.5	32	32	8

Note: H= excavation depth, B= excavation width and L= excavation length and d=Struts spacing.

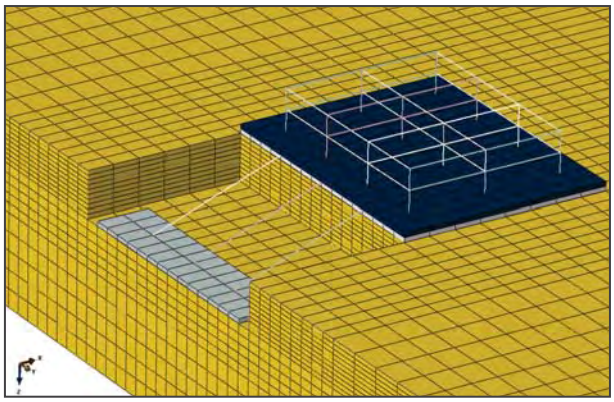

Figure 10. The cut of the 3D model with details.

Fig.11 compares the distribution of the lateral stresses in the soil in the analyses with and without the installation of struts. The direction of the lateral stress is shown in Figs. 11. The positive values represent the tensile stresses. The results show that the distribution of lateral stresses is considerably changed in the ground surface adjacent to the excavation and in the excavation face by the installation of struts. Also, it can be seen that the lateral stress generally decreases near the struts. This is probably due to the arching effect of the struts. It is clear that the arch formation is noticeable in the vicinity of the corner struts. According to many studies [5], [11], [13], [14], [15], [16] due to the arching effect, the horizontal deflection and the vertical settlement near the corners are very small. The parametric analyses and the field-observation results imply that the installation of struts has a similar effect as the diaphragm wall corners.

The contour of plastic strains is depicted in Fig. 12. The evolution of the plastic strains in all of parametric studies shows that the plastic zone begins to form near the bottom of excavation face at the middle of the excavation length.

(a)

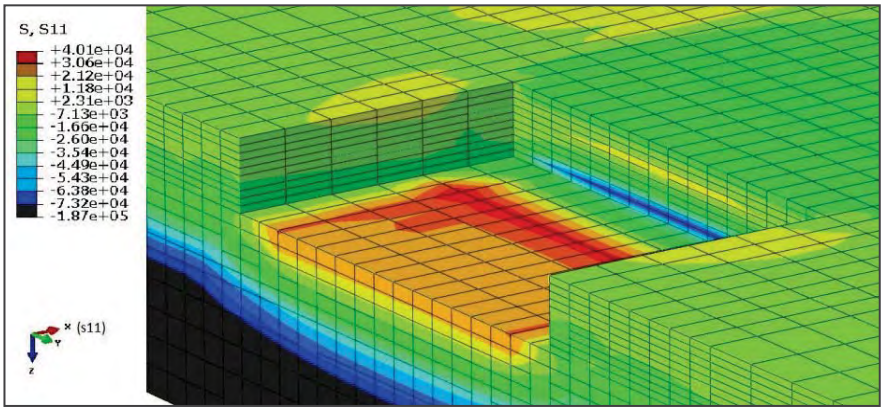

(b)

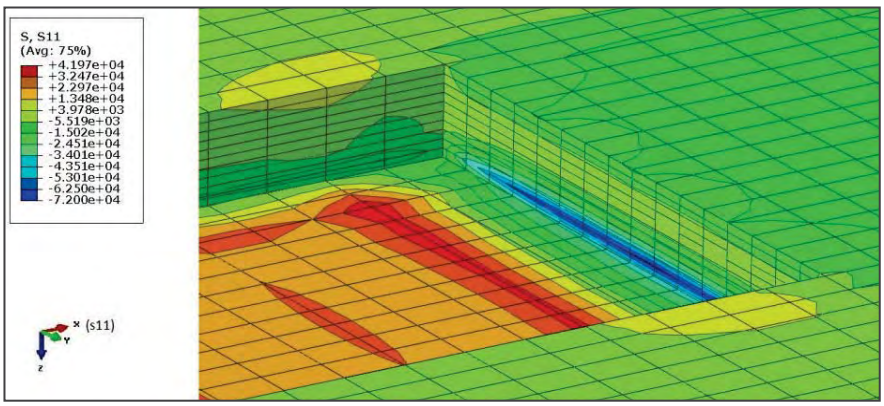

Figure 11. Contours of the soil lateral stresses (a) without struts, (b) with installation of struts.

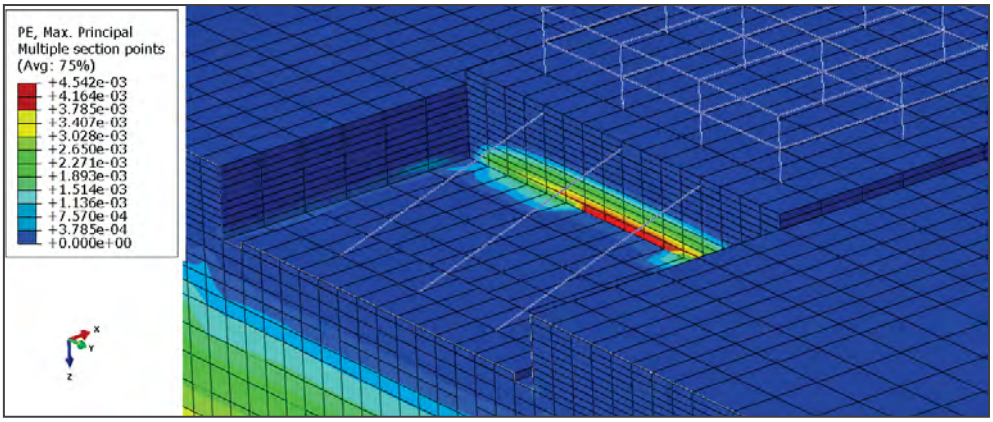

Figure 12. Contours of the soil plastic strains at the final stage of excavation.

4.2 Strut intervals

In order to investigate the effect of the strut intervals at different depths of the excavations and to obtain comparable results in the parametric studies, as mentioned previously, the lengths of the excavations are increased to 32 m in the analyses. The influence of the distance between the struts on the maximum lateral deflections is shown in Fig. 13, where the maximum lateral deformations (δ_{hmax}) are normalized with respect to the depth of the excavation (H). It should be noted that the values at d=0 m are obtained from a two-dimensional analysis. Fig. 13 shows how δ_{hmax}/H increases as the distance between the struts (d) increases, with the influence of the support spacing being more pronounced in the deeper excavation than in the shallower excavation. Fig.13 also shows that when the distance between the struts exceeds the excavation depth, e.g., d/H > 1.0, the δ_{hmax}/H remained approximately constant for a specific excavation depth. These results imply that if the distance between the struts exceeds the excavation depth, the inclined struts would have a minor restraining effect on the horizontal deflections. Consequently, it can be concluded that the maximum distance between the struts should be limited to the excavation depth.

Fig.14 shows the influence of the distance between the struts on δ_{htop}/H and δ_{vtop}/H, of which δ_{htop} and δ_{vtop} are the horizontal and vertical deflections at the top of the ,excavation respectively, and they are obtained from the values of horizontal and vertical deflections near the connection point of the struts to the building. The results show that δ_{htop}/H and δ_{vtop}/H increase with the increasing distance between the struts and the values of δ_{htop}/H and δ_{vtop}/H are seriously affected by the distance between the struts. The above observations can be explained by the fact that the top of the excavation near the connection point of the struts to the building is directly restrained from movement by the struts, and the inclined struts have a serious restraining effect near the excavation surface and also on the adjacent building.

The spacing of the struts can affect their bearing load. To investigate the effect of the interval of the struts on the strut loads, variations of the maximum computed strut load for four excavation depths are shown in Fig.15. The figure shows that the strut load values increase approximately linearly with an increasing distance between the struts for a specific depth. Also, it can be seen from Fig.15 with increasing excavation depth, the strut load increases dramatically.

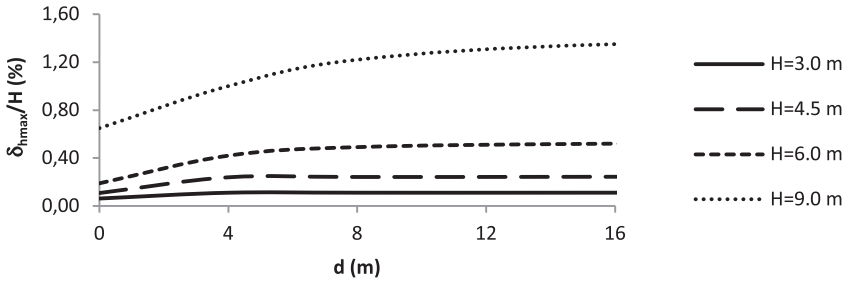

Figure 13. Relationship between the maximum horizontal deflection and the strut intervals for different excavation depths.

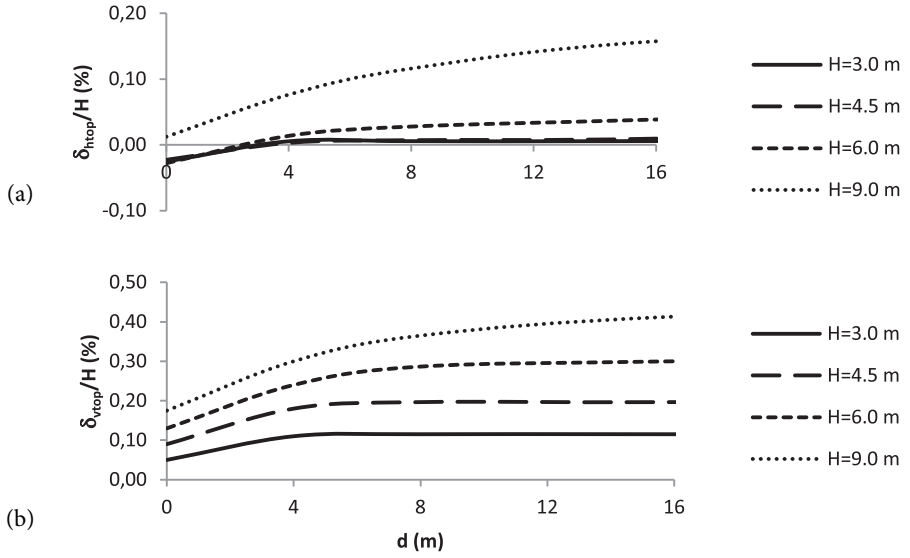

Figure 14. Relationship between the deflections at the point of connection of struts to the building and the strut intervals for different excavation depths, (a) horizontal deflection, (b) vertical deflection.

For an assessment of the effect of the strut intervals on the performance of the struts, the parameter load bearing ratio (LBR) is defined in this study. This parameter is obtained by dividing the unit load of the strut on the unit load of adjacent structures, as shown in Eq.1:

$$LBR = \frac{q_{strut}}{q_{build}} \quad ; \quad q_{strut} = \frac{F_{strut}}{H \cdot d} \qquad (1)$$

where F_{strut} is the strut load, d is the distance between the struts, H is the excavation depth and q_{build} is the unit

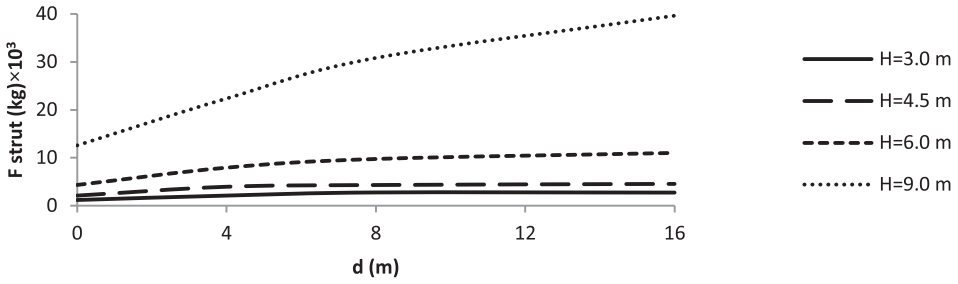

Figure 15. Relationship between the maximum struts load and the strut intervals for different excavation depths.

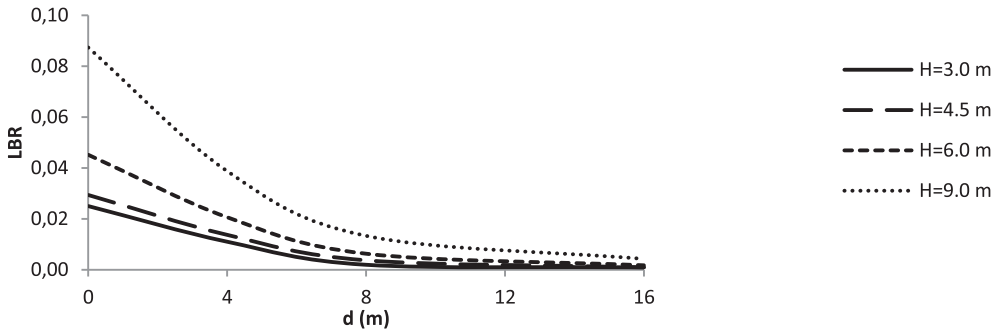

Figure 16. Relationship between the load bearing ratio (LBR) and the strut intervals for different excavation depths.

load of the adjacent building. It assumes that a surcharge of 1 ton/m^2 for each floor of the neighboring buildings act on the ground surface. A greater LBR value implies that the struts have more effect in the bearing building load and vice versa. To consider the effect of the interval of the struts on the LBR, variations of the LBR computed with the maximum strut load for four excavation depths are shown in Fig.16. The results show that LBR decreases rapidly with an increasing distance between the struts for a specific depth. The decrease in LBR is approximately proportional to the square of the struts' interval.

These results indicate that with an increasing distance between the struts, although the struts' loads increase while the load bearing ratio of strut decreases, the performance of the struts in carrying the buildings' loads reduces.

4.3 Strut-installation pattern

As mentioned in the introduction, Sadeghian and Fakher [2] used a numerical analysis to investigate the effect of the strut-installation pattern in two-dimensional excavations. In this paper the efficient sequences of strut installation in 3D excavations are studied. The most effective method in the installation pattern of struts, Fig.2 (e), is selected based on the Sadeghian and Fakher studies [2] and extended in 3D analyses with four different patterns. In all of these patterns, the first stage is the same and is consistent with the method that is illustrated in Fig.1.

(i) Configuration 1: The excavation is executed in one stage, as shown in Fig.1(b); afterwards all of the struts are installed simultaneously, as shown in Fig.1(c) and finally the marginal soil is excavated, as illustrated in Fig.1(d).
(ii) Configuration 2: First the site's excavation zone is fully excavated (Fig.1(b) and Fig.1(d)) and all of the struts are then installed.
(iii) Configuration 3: First corner struts are installed and the marginal soil behind the struts is excavated and then the middle struts are installed and the remaining soil is excavated.
(iv) Configuration 4: Middle struts are installed and the marginal soil in the struts back is excavated. Then the corner struts are installed and the remaining soil is excavated.

To find the most effective configuration, horizontal deflections are considered. Fig.17 compares the excavation-induced maximum horizontal deflection along the excavation length for the four mentioned excavation procedures. It should be noted that the results in Fig.17 are obtained from the numerical model with the parameters as given in Table.4. According to Fig.17 the maximum horizontal displacement in the center of the excavation length induced by configuration 2 is larger than the other configuration and the most effective configuration is configuration 1. In configuration 4, since the middle struts are installed earlier than the corner struts, the horizontal deflection at the middle of the excavation length is restrained rather than the other configurations. Obviously, the most efficient method of installation for the strut is the installation of all the struts simultaneously. But if it is not possible to execute all of struts installation in one step, the installation of the middle struts at first and then the installation of the corner struts produces fewer horizontal deflections at the middle of the excavation length.

5 DISPLACEMENT-BASED DESIGN

Limiting the movements of adjacent buildings is becoming a significant design issue because deformations can cause significant damage to the structures. Increasingly, designs are controlled by the need to limit movements,

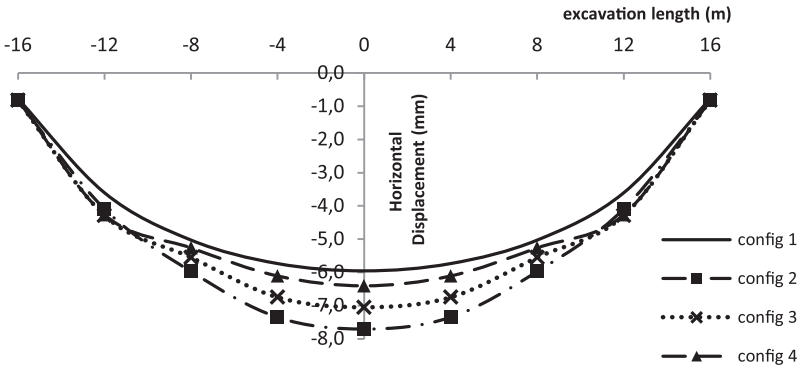

Figure 17. Comparison of the maximum horizontal deflection along the excavation length for four strut installation configurations.

which goes beyond the traditional design approach of focusing on the required support loads and avoiding collapse. These conditions require a new approach to designing support systems to focus on controlling displacements [28]. In the displacement-based design, a comprehensive understanding of the characteristics of deformations is very important. Using a displacement-based design approach requires a way to predict displacements. The proposed approach determines the displacement based on numerical studies and compares the results with the allowable displacement.

5.1 Allowable deflections

There are several publications on the allowable deflections for different types of structures and some criteria have been proposed for estimating the potential of damage to adjacent buildings. Boscardin and Cording [4] developed a plot relating the angular distortion and horizontal strain to building damage. The establishing permissible deflections range depends on the project conditions. The maximum allowable angular distortion and the horizontal strain should be determined according to the level of damage and the type and condition of the building. The values for the maximum allowable horizontal (δ_h) and vertical (δ_v) deflections can then be obtained.

5.2 Simple estimation of deflections

The deformations are the result of many complex factors such as ground condition, type of retaining structure, stiffness of supports and adjacent building conditions. The deflections determination can be obtained from a dimensional analysis of the parameters that appeared to contribute to the deflections in an excavation. The parameters that have the most effect on the deflections are as follows:

$$\delta_h = f(E_s, E_b, H, \gamma_s, c, n, K_{st}) \qquad (2)$$

$$\delta_v = f(E_s, E_b, H, \gamma_s, c, n, K_{st}) \qquad (3)$$

where δ_h and δ_v are the horizontal and vertical deflections, respectively, and E_s = Young's modulus of the soil; E_b = Young's modulus of the structure; H = excavation depth; γ_s = unit weight of the soil; c = cohesion of the soil; n is the number of the story of building; and K_{st} is the stiffness of the strut and is obtained by:

$$K_{st} = \frac{A_{st} E_{st}}{ld} \qquad (4)$$

where A_{st} = cross-sectional area of strut; E_{st} = modulus of elasticity of strut; l = length of strut; and d = distance between struts.

A dimensional analysis suggests that a dimensionally homogeneous equation can be reduced to a relationship among a complete set of dimensionless products. The correct use of the dimensionless products makes the parametric studies more efficient by revealing which variables are truly independent [29]. From an inspection of the variables contributing to deflections, it can be seen that three dimensionless groupings emerge. One grouping is the relative stiffness resistance, $E_b \cdot E_{st} / E_s \cdot K_{st}$, which captures the soil-structure-strut interaction [30]. Another grouping is the excavation stability number, $H\gamma_s / c$, which characterizes the effects of the soil conditions. The third dimensionless parameter is the number of the story of the building (n). The two first-mentioned dimensionless groupings are combined and produce the dimensionless parameter R as:

$$R = \left(\frac{E_b}{E_s} \cdot \frac{E_{st}}{K_{st}}\right) \times \frac{H\gamma_s}{c} \quad \text{or} \quad R = \left(\frac{E_b}{E_s} \cdot \frac{ld}{A_{st}}\right) \times \frac{H\gamma_s}{c} \qquad (5)$$

Thus Equations 2 and 3 can be rewritten as:

$$\delta_h = f(R,n) \qquad (6)$$

$$\delta_v = f(R,n) \qquad (7)$$

It should be noted that all the variables included in the dimensionless parameters are from basic soil, geometry parameters of excavation and adjacent building that the designer can easily determine from standard soil tests and excavation and building specifications; and also the struts' cross-sectional area and materials as design parameters can be estimated primarily based on similar excavation projects.

Fig.18 shows the dimensionless parameter (R,n) values and the maximum deflections obtained from the parametric finite-element studies and the fitted curves.

The trend curves fitted through the parametric data have the form:

$$\frac{\delta_{htop}}{H}(\%) = 0.42e^{0.5n} \times \left[\left(1.54\times10^{-20} \times R^2\right) + \left(1.7\times10^{-11} \times R\right) + \left(5.1\times10^{-3}\right)\right] \qquad (8)$$

$$\frac{\delta_{vtop}}{H}(\%) = 1.01e^{0.5n} \times \left[\left(2.9\times10^{-20} \times R^2\right) + \left(1.65\times10^{-10} \times R\right) + \left(0.13\right)\right] \qquad (9)$$

$$\frac{\delta_{h\max}}{H}(\%) = 0.93e^{0.1n} \times \left[\left(1.51\times10^{-19} \times R^2\right) + \left(1.68\times10^{-10} \times R\right) + \left(0.19\right)\right] \qquad (10)$$

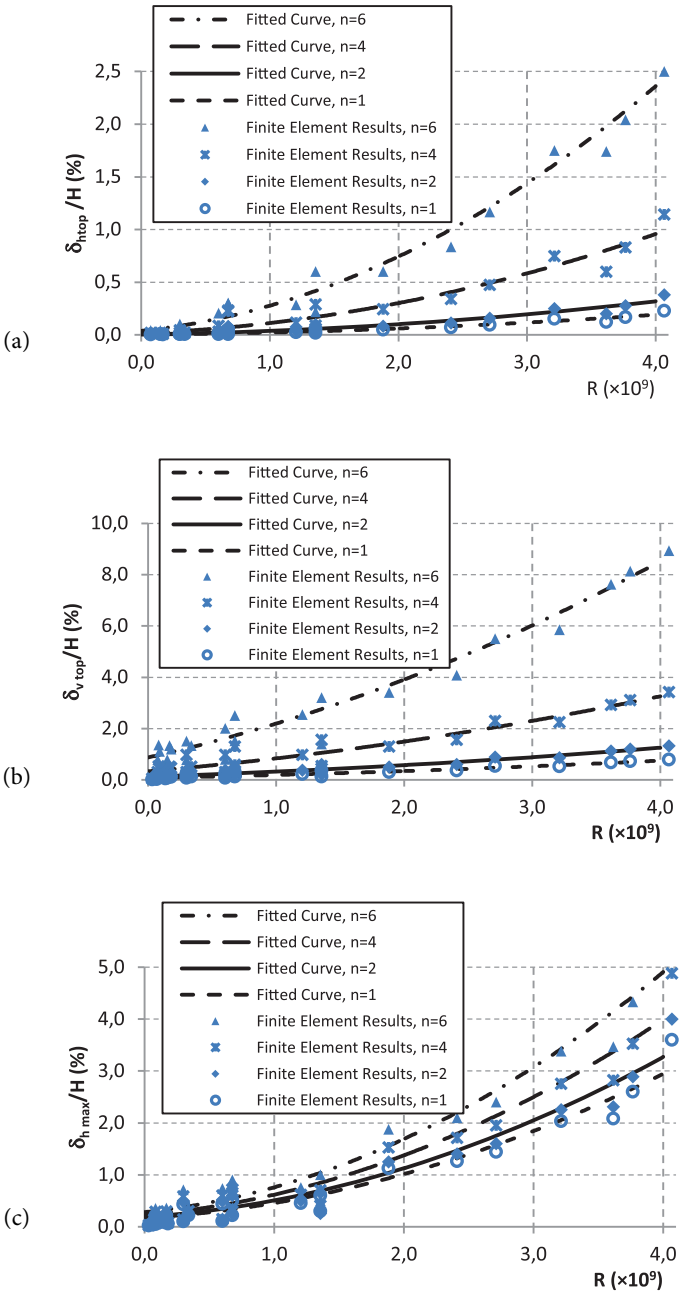

Figure 18. Comparison of the finite-element parametric studies with the proposed relations; (a) horizontal deflection at the top of the excavation, (b) vertical settlement at the top of the excavation, (c) maximum lateral deflection of the excavation face.

Eq.8 to 10 develop a design chart that allows the designer to choose the appropriate struts' cross-sectional area (A_{st}) and the distance between the struts (d) based on the design criteria of limiting the deformations. Conversely, for a given struts cross-sectional area and the distance between the struts, Eq.8 to 10 allow the designer to predict the horizontal and vertical deflections for excavations supported by inclined struts based on simple soil data and excavation geometry.

5.3 Proposed design guidelines

Based on the results of the current study, the following design guidelines are offered for estimating the design parameters.

1. Determine the soil and structure condition, including material properties (E_s, E_b, γ_s, c) and excavation and structure geometry (H, n).

2. Choose the cross-sectional area and the inclination angle of struts, based on the recommendations which are proposed in the introduction of paper; choose the distance between the struts based on the recommendations that are proposed in Section 4.2; calculate the struts stiffness (K_{st}).
3. Determine the values of allowable deflections as described in Section 5.1.
4. The maximum deflections can be obtained using all the input parameters from Eq. 8 to 10. The value of the deflections should then be compared with the allowable deflection to ensure that they are within acceptable limits. If the values of the deformations are not within permissible limits, the strut stiffness parameter should be adjusted to ensure that the deflections are within reasonable limits.

6 CONCLUSIONS

This study investigated the effect of struts on the deflections in excavations using a series of 3D finite-element parametric studies using strut spacing and the configuration of the strut installation as variables. The influence of the strut installation on the excavation was also studied. The results can be used to approximate the design of reasonable strut intervals and their cross-sectional areas. This study confirmed the proposed performance mechanism for inclined struts using field observations and 3D numerical analysis results. Finally a performance design approach was presented that can be used to effectively design inclined struts for an excavation based on the deformation limits. The following were observed:

1. The use of inclined struts connected to adjacent buildings decreased the amount of deformation and created a corner effect similar to that for diaphragm wall corners; the deflections at the corners were much smaller in response to the arching effect. The deflections were also smaller in the section where the struts were installed than in the sections that were some distance from the struts.
2. The use of inclined struts strongly decreased the horizontal deformation near the ground surface around the contact point of the strut and lowered the location of the maximum wall deformation to a point near the bottom of the excavation. Whereas, large horizontal deformations occurred near the surface of the excavation without the use of struts.
3. The stress distribution pattern outside the excavation zone at the ground surface revealed that the lateral stresses decreased near the struts in response to the arching effect of the struts; an arch formation was noticeable in the vicinity of the corner struts. The evolution of plastic strains in the excavations showed that a plastic zone began to form near the bottom of the excavation face in the middle of the excavation length.
4. Horizontal deflections increased as the strut intervals increased. It was found that the maximum spacing between the struts should not exceed the excavation depth.
5. The load bearing ratio (LBR) was defined and used to assess the effect of strut intervals on the performance of the struts. This parameter was obtained by dividing the unit load of a strut by the unit load of the adjacent structures. A larger LBR indicates that the struts play a major role in bearing the load from a building. The load on the struts increases as the distance between the struts increases, but the load bearing ratio (LBR) decreases and the role of the struts in carrying the building loads decreases. The decrease in LBR is approximately proportional to the square of the interval between the struts.
6. The most efficient strut-installation sequence in the length of the excavation that produces the greatest decrease in the horizontal deflection is the simultaneous installation of struts. If it is not possible to execute the installation of all the supports at the same time, the middle struts should be installed first and then the corner struts.

REFERENCES

[1] Fakher, A., Sadeghian, S, 2011. An investigation into Inclined Struts method as a type of shoring. Geotechnical Aspects of Underground Construction in Soft Ground, Rome, Italy, 369–375. DOI: 10.1201/b12748-48

[2] Sadeghian, S., Fakher, A. 2010. An investigation into a shoring method to support buildings adja¬cent to excavations. The 17th Southeast Asian Geotechnical Conference Proceeding, Taipei, Taiwan, May 10-13, pp. 207-210.

[3] Sabzi, Z., Fakher, A. 2015. The performance of buildings adjacent to excavation supported by inclined struts. International Journal of Civil Engineering 13, 1, 1-15.

[4] Boscardin, M.D., Cording, E.G. 1989. Building response to excavation-induced settlement. Journal of Geotechnical Engineering 115, 1, 1-21. DOI: 10.1061/(ASCE)0733-9410(1989)115:1(1)

[5] Lee, F.H., Yong, K.Y., Quan, K.C.N., Chee, K.T. 1998a. Effect of corners in strutted excavations: Field monitoring and case histories. J. Geotech. Geoenviron. Eng. 124, 4, 339–349. DOI: 10.1061/(ASCE)1090-0241(1998)124:4(339)

[6] Lee, F.H., Yong, K.Y., Lee, S.L., Toh, C.T. 1989b. Finite element modelling of strutted excavation.

Numerical models in geomechanics, Elsevier Applied Science, London, U.K., 577-584.
[7] Yong, K.Y., Lee, F.H., Parnploy, U., Lee, S.L. 1989. Elasto-plastic consolidation analysis for strutted excavation in clay. Computer and Geotechnics 8. 311-328. DOI: 10.1016/0266-352X(89)90038-4
[8] Finno, R.J., Harahap, I.S. 1991. Finite element analysis of HDR-4 excavation. Journal of Geotechnical and Geoenvironmental Engineering 117, 10, 1590–1609. DOI: 10.1061/(ASCE)GT.1943-5606.0001533
[9] Smith, I.M., Ho, D.K.H. 1992. Influence of construction technique on the performance of a braced excavation in marine clay. Int.J. Numer. and Analytical Methods in Geomech. 16, 845-867. DOI: 10.1002/nag.1610161202
[10] Coutts D.R, Wang J., Cai, J.G. 2001. Monitoring and analysis of results for two strutted deep excavations using vibrating wire strain gauges. Tunneling and Underground Space Technology 16, 2, 87-92. DOI: 10.1016/S0886-7798(01)00032-3
[11] Finno, R.J., Roboski, J.F. 2005. Three-dimensional responses of a tied-back excavation through clay. J. Geotech. Geoenviron. Eng. 131, 3, 273–282. DOI: 10.1061/(ASCE)1090-0241(2005)131:3(273)
[12] Ou, C.Y, Shiau, B.Y. 1998. Analysis of the corner effect on excavation behaviors. Can. Geotech. J. 35, 532-540.
[13] Ou, C.Y., Chiou, D.C., Wu, T.S. 1996. Three-dimensional finite element analysis of deep excavations. J. Geotech. Eng. 12, 5, 337–345.
[14] Ou, C.Y., Hsieh, P. G., Lin, Y.L. 2011. Performance of Excavations with Cross Walls. J. Geotech. Geoenviron. Eng. 137, 1, 94-104. DOI: 10.1061/(ASCE)GT.1943-5606.0000402
[15] Wu, C.H., Ou, C.Y., Tung, N. 2010. Corner effects in deep excavations establishment of a forecast model for taipei basin T2 zone. Journal of Marine Science and Technology 18, 1, 1-11.
[16] Blackburn, J.T., Finno, R.J. 2007. Three-dimensional responses observed in an internally braced excavation in soft clay. J. Geotech. Geoenviron. Eng. 133, 11, 1364–1373. DOI: 10.1061/(ASCE)1090-0241(2007)133:11(1364)
[17] Finno, R.J., Blackburn, J.T., Roboski, J.F. 2007. Three-dimensional effects for supported excavations in clay. J. Geotech. Geoenviron. Eng. 133, 1, 30–36. DOI: 10.1061/(ASCE)1090-0241(2007)133:1(30)
[18] Sabzi, Z., Fakher, A. 2012. The effect of confining stress on the analysis of excavations adjacent to existing buildings. International Conference on Geotechnique, Construction Materials and Environment, Kuala Lumpur, Malaysia, Nov 14-16, pp. 162-166.
[19] Hibbit, Karlsson, Sorensen, Inc., 2010. ABAQUS/Standard User's Manual, Version 6.10. Pawtucket, RI, USA.
[20] Brown, P.T., Booker, J.R. 1985. Finite element analysis of excavation .Computers and Geotechnics 1: 207.220.
[21] Duncan, J.M., Chang, C.Y. 1970. Nonlinear analysis of stress and strain in soils. Journal of the Soil Mechanics and Foundations Division, ASCE, 96, 5, 637-659.
[22] Khoiri, M., Ou, C.Y. 2013. Evaluation of deformation parameter for deep excavation in sand through case histories. Computers and Geotechnics 47, 57–67. DOI: 10.1016/j.compgeo.2012.06.009
[23] Dang, H., Lin, H., Juang, C. 2014. Analyses of braced excavation considering parameter uncertainties using a finite element code. Journal of the Chinese Institute of Engineers 37, 2, 141-151. DOI: 10.1080/02533839.2013.781790
[24] Dang, H., Lin, H., Juang, C. 2012. Evaluation of soil variability influence on deep excavation analysis–simplified approach. GeoCongress, pp. 2895-2903. DOI: 10.1061/9780784412121.296
[25] Verghese, S.J., Nguyen, C.T., Bui, H.H. 2013. Evaluation of plasticity-based soil constitutive models in simulation of braced excavation. Int. J. of GEOMATE. 5, 2, 672-677.
[26] Wong, K.S., Broms, B.B. 1989. Lateral deflection of braced excavation in clays. Journal of Geotechnical Engineering, ASCE, 115, 6, 853-870. DOI: 10.1061/(ASCE)0733-9410(1989)115:6(853)
[27] Duncan, J.M., Byrne, P., Wong, K.S, Mabry, P. 1980. Strength, stress-strain and bulk modulus parameters for finite element analysis of stresses and movements in soil masses. Report No. UCB/GT/80-01, College of Engineering, Office of Research Services, University of California, Berkley, Calif.
[28] Marr, W.A., Hawkes, M. 2010. Displacement-based design for deep excavations. ASCE, Earth Retention Conference 3: pp. 82-100. DOI: 10.1061/41128(384)6.
[29] Wood, M.D. 2004. Geotechnical Modelling. Spon, London.
[30] Sebastian B.L., Zapata-Medina, D.G. 2012. Method for estimating system stiffness for excavation support walls. J. Geotech. Geoenviron. Eng.138, 1104-1115. DOI: 10.1061/(ASCE)GT.1943-5606.0000683